

Liquid-phase synthesis of Li_2S and Li_3PS_4 with lithium-based organic solutions

Jieru Xu(许洁茹), Qiuchen Wang(王秋辰), Wenlin Yan(闫汶琳), Liquan Chen(陈立泉), Hong Li(李泓), and Fan Wu(吴凡)

Citation: Chin. Phys. B, 2022, 31 (**9**): 098203. DOI: 10.1088/1674-1056/ac7459
Journal homepage: http://cpb.iphy.ac.cn; http://iopscience.iop.org/cpb

What follows is a list of articles you may be interested in

Configurational entropy-induced phase transition in spinel $LiMn_2O_4$

Wei Hu(胡伟), Wen-Wei Luo(罗文崴), Mu-Sheng Wu(吴木生), Bo Xu(徐波), and Chu-Ying Ouyang(欧阳楚英)
Chin. Phys. B, 2022, 31 (**9**): 098202. DOI: 10.1088/1674-1056/ac6863

Probing component contributions and internal polarization in silicon-graphite composite anode for lithium-ion batteries with an electrochemical-mechanical model

Yue Chen(陈约), Fuliang Guo(郭福亮), Lufeng Yang(杨陆峰), Jiaze Lu(卢嘉泽), Danna Liu(刘丹娜), Huayu Wang(王华宇), Jieyun Zheng(郑杰允), Xiqian Yu(禹习谦), and Hong Li(李泓)
Chin. Phys. B, 2022, 31 (**7**): 078201. DOI: 10.1088/1674-1056/ac6012

Lithium ion batteries cathode material: V_2O_5

Baohe Yuan(袁保合), Xiang Yuan(袁祥), Binger Zhang(张冰儿), Zheng An(安政), Shijun Luo(罗世钧), and Lulu Chen(陈露露)
Chin. Phys. B, 2022, 31 (**3**): 038203. DOI: 10.1088/1674-1056/ac21be

Analysis on diffusion-induced stress for multi-layer spherical core-shell electrodes in Li-ion batteries

Siyuan Yang(杨思源), Chuanwei Li(李传崴), Zhifeng Qi(齐志凤), Lipan Xin(辛立攀), Linan Li(李林安), Shibin Wang(王世斌), and Zhiyong Wang(王志勇)
Chin. Phys. B, 2021, 30 (**9**): 098201. DOI: 10.1088/1674-1056/ac11de

In situ formed FeS_2@CoS cathode for long cycling life lithium-ion battery

Xin Wang(王鑫), Bojun Wang(汪博筠), Jiachao Yang(杨家超), Qiwen Ran(冉淇文), Jian Zou(邹剑), Pengyu Chen(陈鹏宇), Li Li(李莉), Liping Wang(王丽平), and Xiaobin Niu(牛晓滨)
Chin. Phys. B, 2021, 30 (**8**): 088201. DOI: 10.1088/1674-1056/abe9ab

---

RAPID COMMUNICATION

Liquid-phase synthesis of Li_2S and Li_3PS_4 with lithium-based organic solutions

Jieru Xu(许洁茹)[1,2,3,4], Qiuchen Wang(王秋辰)[1,2], Wenlin Yan(闫汶琳)[1,2,3,4], Liquan Chen(陈立泉)[1,2,3,4], Hong Li(李泓)[1,2,3,4], and Fan Wu(吴凡)[1,2,3,4,5,†]

[1] *Key Laboratory for Renewable Energy, Beijing Key Laboratory for New Energy Materials and Devices, Beijing National Laboratory for Condensed Matter Physics, Institute of Physics, Chinese Academy of Sciences, Beijing* 100190, *China*

[2] *University of Chinese Academy of Sciences, Beijing* 100049, *China*

[3] *Tianmu Lake Institute of Advanced Energy Storage Technologies, Liyang* 213300, *China*

[4] *Yangtze River Delta Physics Research Center, Liyang* 213300, *China*

[5] *Nano Science and Technology Institute, University of Science and Technology of China, Suzhou* 215123, *China*

(Received 7 May 2022; revised manuscript received 25 May 2022; accepted manuscript online 29 May 2022)

Sulfide solid electrolytes are widely regarded as one of the most promising technical routes to realize all-solid-state batteries (ASSBs) due to their high ionic conductivity and favorable deformability. However, the relatively high price of the crucial starting material, Li_2S, results in high costs of sulfide solid electrolytes, limiting their practical application in ASSBs. To solve this problem, we develop a new synthesis route of Li_2S via liquid-phase synthesis method, employing lithium and biphenyl in 1, 2-dimethoxyethane (DME) ether solvent to form a lithium solution as the lithium precursor. Because of the comparatively strong reducibility of the lithium solution, its reaction with sulfur proceeds effectively even at room temperature. This new synthesis route of Li_2S starts with cheap precursors of lithium, sulfur, biphenyl and DME solvent, and the only remaining byproduct (DME solution of biphenyl) after the collection of Li_2S product can be recycled and reused. Besides, the reaction can proceed effectively at room temperature with mild condition, reducing energy cost to a great extent. The as-synthesized Li_2S owns uniform and extremely small particle size, proved to be feasible in synthesizing sulfide solid electrolytes (such as the solid-state synthesis of Li_6PS_5Cl). Spontaneously, this lithium solution can be directly employed in the synthesis of Li_3PS_4 solid electrolytes via liquid-phase synthesis method, in which the centrifugation and heat treatment processes of Li_2S are not necessary, providing simplified production process. The as-synthesized Li_3PS_4 exhibits typical Li^+ conductivity of 1.85×10^{-4} S·cm^{-1} at 30 °C.

Keywords: lithium sulfide, sulfide solid electrolyte, liquid phase synthesis, lithium-based organic solution

PACS: 82.47.Aa, 65.40.gk, 82.45.Gj **DOI:** 10.1088/1674-1056/ac7459

1. Introduction

All-solid-state batteries (ASSBs) are widely recognized as as one of the the most promising next-generation energy storage technologies to balance properties of high energy density, high power density, high safety and broadened working temperature range.[1] Among basic routes of ASSBs, sulfide solid electrolyte (SE) is widely recognized as the most promising one due to its high ionic conductivity[2–4] and favorable deformability.[5] Aiming to bridge the great gap between lab-scale fabrication and industrial large-scale production of sulfide-based ASSBs, the mass production of sulfide solid electrolytes is one of the most overwhelming issues. High-temperature solid state reaction[2–4] and mechanochemical method[6–8] are typical conventional solid-phase synthesis methods of sulfide solid electrolytes with relatively high-energy cost in high-temperature heat treatment process[2–4,9–11] and high-energy ball milling process.[6–8] Recently, liquid-phase synthesis method has been widely reported, which can be an effective way for large-scale production of sulfide SEs with decreasing energy costs attributable to its mild reaction conditions. Taking the synthesis of Li_3PS_4 as an example, which is one of the most studied sulfide solid electrolytes in the field of liquid phase synthesis since Liang *et al.* firstly synthesized nanoporous β-Li_3PS_4 by a wet-chemical method in 2013.[12] In a typical synthesis, Li_2S and P_2S_5 with a stoichiometry of 3:1 were mixed in anhydrous tetrahydrofuran (THF), followed by overnight stirring at room temperature and subsequent centrifugation to obtain Li_3PS_4·3THF precipitation. After the removal of THF at 80 °C and further heating at 140 °C, crystalline β-Li_3PS_4 with ionic conductivity of 1.6×10^{-4} S·cm^{-1} at 25 °C was synthesized. Liang *et al.* also employed acetonitrile (ACN) to synthesize β-Li_3PS_4 nanoflakes,[13] and synthesized Li_3PS_4 electrolytes with shape-controlled plate-like morphology via a special exchange process from THF to ACN solvent.[14] Except for the special morphology, the particle size of sulfide solid electrolytes can be mediated by controlling parameters (especially the solvent type) of liquid-phase synthesis. For instance, $75Li_2S{\cdot}25P_2S_5$ solid electrolytes with small and uniform particle sizes (2.2±1.68 μm) were synthesized

†Corresponding author. E-mail: fwu@iphy.ac.cn

© 2022 Chinese Physical Society and IOP Publishing Ltd

with the participation of anhydrous dibutyl ether.[15] The as-prepared $75Li_2S{\cdot}25P_2S_5$ SEs exhibited ionic conductivity of about 3.1×10^{-4} S·cm^{-1} at room temperature, with small and uniform particle sizes, which can form intimate contact with active materials. However, even with the liquid-phase synthesis method, the costs of sulfide solid electrolytes are relatively high, considering the relatively high price of the crucial starting material, Li_2S. Common synthesis methods of Li_2S are summarized as follows. Carbothermic reduction of Li_2SO_4 is a predominant commercial synthesis method. Specifically, Li_2SO_4 is reduced with the oxidation of carbon during the reaction of molten Li_2SO_4 and carbon at high temperature of 1000 °C, with high energy cost and the release of CO_2 harmful gas.[16] An acid-base reaction at the temperature of 130–445 °C is another synthesis route of Li_2S, in which Li_2CO_3 or LiOH are lithium precursors and H_2S is used as the sulfur precursor. However, the formation of Li–S–O impurities needs additional purifying process via organic solvents.[17,18] Therefore, a new route for Li_2S synthesis is eagerly expected, which is expected to have cheap precursors, mild reaction conditions and environmentally friendly and easily separated byproducts. Alkali metal (such as Li, Na and K) has been reported to react with certain aromatic hydrocarbons in ether solvent to form an alkali solution at room temperature since 1900s.[19] Such solutions, containing radical anions, can be used as reducing agents in chemical synthesis.[20,21] In this work, lithium reacts with biphenyl in 1, 2-dimethoxyethane (DME) ether solvent to form a lithium solution at room temperature, which can react with sulfur at high reaction kinetics even at room temperature. This new synthesis route of Li_2S starts with cheap precursors of lithium, sulfur, biphenyl and DME solvent, and the only remaining byproduct (DME solution of biphenyl) after the collection of Li_2S product can be recycled and reused. Besides, the reaction can proceed effectively at room temperature with mild condition, reducing energy cost to a great extent. The as-synthesized Li_2S owns uniform and extremely small particle size, proved to be feasible in synthesizing sulfide solid electrolytes (such as the solid-state synthesis of Li_6PS_5Cl). Spontaneously, this lithium solution can be directly employed in the synthesis of Li_3PS_4 solid electrolytes via liquid-phase synthesis method, in which the centrifugation and heat treatment processes of Li_2S are not necessary, providing simplified production process. The as-synthesized Li_3PS_4 exhibits typical Li^+ conductivity of 1.85×10^{-4} S·cm^{-1} at 30 °C.

2. Experiment

2.1. Materials synthesis

2.1.1. Synthesis of Li_2S

The synthesis process of Li_2S is illustrated in Fig. 1(a). First, lithium-based organic liquid metal solution was prepared as the lithium source. Specifically, an aromatic hydrocarbon, biphenyl (Alfa, 99%), was fully dissolved in extra DME (Energy Chemical, 99%) solvent at room temperature via a simple string process. A transparent and colorless solution of biphenyl was formed with a concentration of 1 mol·L^{-1}, referred as $Bp_{1.0}(DME)_{1.0}$. Then, lithium metal was cut into pieces (China Energy Lithium Co. Ltd, 99.95%) and put into the $Bp_{1.0}(DME)_{1.0}$ solution, forming a dark-green solution after a 12-h standing at room temperature. The molar ratio between Li and biphenyl was fixed at 1:1, referred as $Li_{1.0}Bp_{1.0}(DME)_{1.0}$. Afterwards, S (50 mol% of lithium, Alfa, 99.5%) was immersed in the $Li_{1.0}Bp_{1.0}(DME)_{1.0}$ complex solution and allowed to react for 12 h during the string at room temperature. The suspension was then centrifugated and washed with DME. The resulting solution turned transparent and colorless, which is supposed to be the DME solution of biphenyl and can be recycled and reused. The resulting solid was yellowish white, then dried under vacuum at 100 °C for 12 h to remove the remaining solvent. Finally, heat treatment at different temperatures for 5 h was carried out to promote the crystallization of Li_2S, obtaining white powder. THF solvent was also employed using the same synthesis process to determine the proper solvent.

2.1.2. Synthesis of Li_6PS_5Cl

Li_6PS_5Cl powder was prepared by conventional solid-state synthesis. A stoichiometric mixture of Li_2S, P_2S_5 (Macklin, 99%) and LiCl (99.9%, Aladdin) was mechanochemically milled for 20 h, followed by heat-treatment at 550 °C for 5 h in a sealed quartz ampoule. Two types of Li_2S were used to synthesis Li_6PS_5Cl, including Li_2S synthesized in this work and commercial Li_2S (Alfa, 99.9%).

2.1.3. Synthesis of Li_3PS_4 via the two-step route and the one-step route

The synthesis processes of Li_3PS_4 via the two-step route and the one-step route are illustrated in Fig. 1(b). First, lithium-based organic liquid metal solution $Li_{1.0}Bp_{1.0}(DME)_{1.0}$ was prepared as the lithium source, same as the first step of Li_2S synthesis. Afterwards, S (Alfa, 99.5%) and P_2S_5 (Macklin, 99%) in stoichiometric proportions were immersed in the $Li_{1.0}Bp_{1.0}(DME)_{1.0}$ complex solution. For the two-step route, S and P_2S_5 were added in batches. S was added first, forming a suspension of Li_2S in Bp-DME solution after 12-h string at room temperature. Then, P_2S_5 was added into the $Li_2S{\cdot}$ Bp· DME suspension and allowed to react for 12 h during string at 80 °C. For the one-step route, S and P_2S_5 were added into the $Li_{1.0}Bp_{1.0}(DME)_{1.0}$ complex solution at one time, followed by a 12-h stirring at 80 °C for adequate reaction. The reaction products via two routes were then centrifugated and washed with DME. The resulting solution turned transparent and colorless, which is supposed to be the DME solution of biphenyl and can be recycled and reused. The resulting solid was then dried under vacuum at 100 °C for 12 h to remove the remaining solvent. Finally, heat treatment at different temperatures for 10 h was carried out to promote the crystallization of Li_3PS_4, obtaining grayish-white powder.

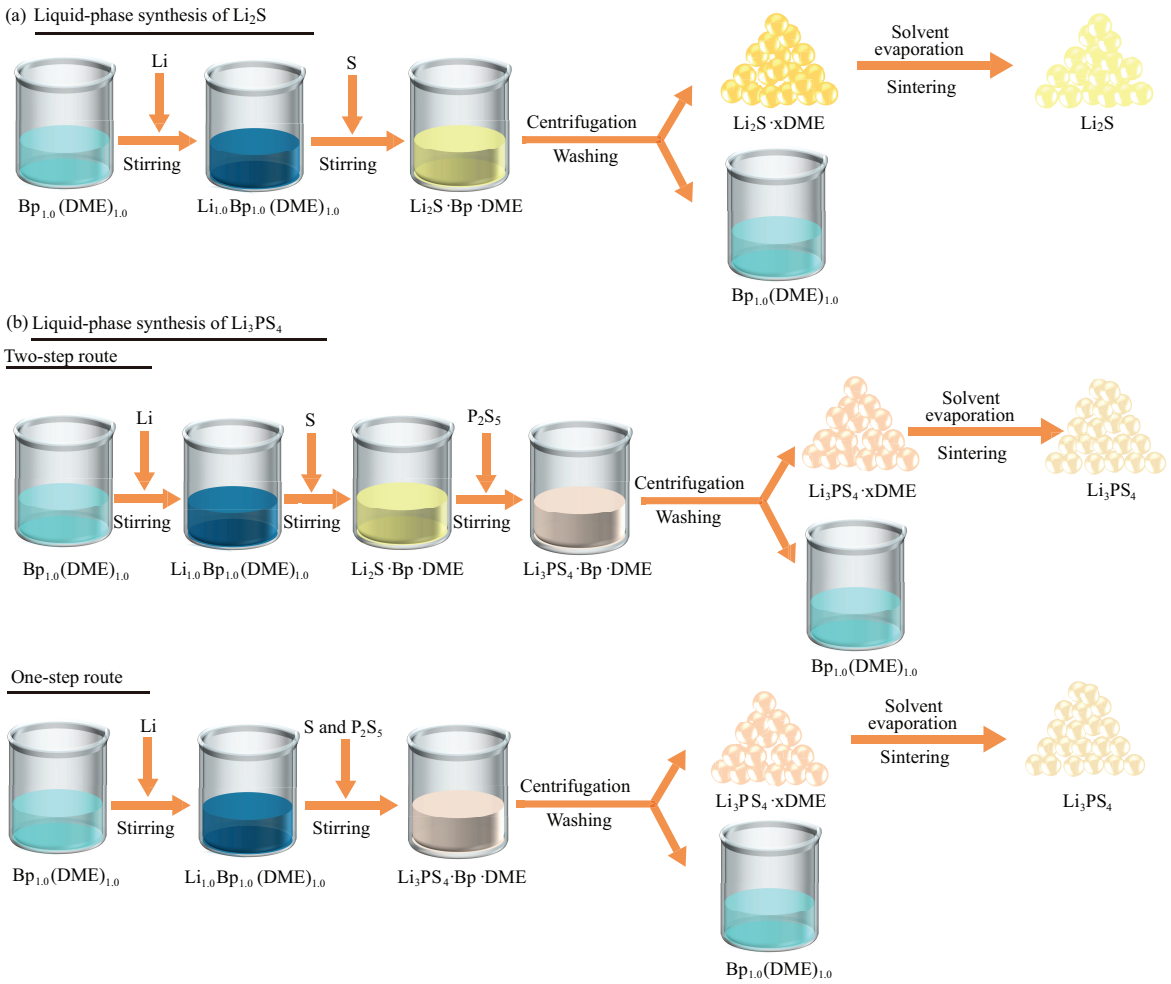


Fig. 1. Schematic illustrations of the synthesis process of (a) Li_2S and (b) Li_3PS_4.

2.2. Structure, morphology and chemistry characterization

The crystal structure of synthesized materials was investigated by x-ray diffraction (XRD, PERSEE XD2) equipped with Cu $K\alpha$ radiation ($\lambda = 1.54178$ Å) operated at 36 kV and 20 mA in the 2θ range of 10°–80°. A field emission scanning electron microscope (SEM, HITACHI, SU8100) was used to characterize the surface morphology of synthesized materials.

2.3. Electrochemical characterization

2.3.1. Ionic conductivities of solid electrolytes

For the measurement of ionic conductivity of solid electrolytes, the testing cells were assembled as follows: 100 mg of sulfide electrolyte was added into a Swagelok model cell and pressed under a pressure of 870 MPa into a pellet, directly using two stainless-steel (SS) rods as ion-blocking electrodes. The as-prepared testing cells were measured by alternating-current (AC) impedance spectroscopy instrument (Zennium Pro Electrochemical Workstation) in the frequency range of 8 MHz–0.1 Hz with an AC amplitude of 20 mV at temperatures ranging from −30 °C to 30 °C with 15 °C steps. The cell was kept at the specific temperature for 2 h prior to the measurement.

Ionic conductivities were calculated using the following equation:

$$\sigma = \frac{1}{R} \cdot \frac{l}{A}, \tag{1}$$

where σ is the ionic conductivity ($S \cdot cm^{-1}$), R is the resistance (Ω), l is the thickness (cm), A is the area (cm^2) of the cold-pressing pellets of solid electrolytes.

2.3.2. Electronic conductivities of solid electrolytes

The electronic conductivities of solid electrolytes were measured via the direct-current (DC) polarization method using Zennium Pro Electrochemical Workstation. The testing cells are the same cells for ionic conductivity testing, which are SS/cold-pressing pellet/SS mold cells assembled under a pressure of 870 MPa. The cell was polarized at DC voltage (ΔV) of 50 mV, and the steady-state current I_s of the cell was recorded. The electronic resistances were obtained from $\Delta V / I_s$ and the corresponding conductivities were calculated using Eq. (1).

2.3.3. Fabrication of ASSBs and electrochemical performance measurements

To prepare the composite cathode of ASSBs, $LiNi_{0.8}Co_{0.1}Mn_{0.1}O_2$ (NCM811), sulfide solid electrolytes, and vapor grown carbon fiber (VGCF, Showa Denko K.K.) were mixed with a weight ratio of 50:45:5 for 30 min. Nano-Si, sulfide solid electrolytes and VGCF were mixed with a weight ratio of 50:45:5 for 30 min to obtain the composite anode powder. The lab-scale ASSBs were fabricated as follows: 1) 2.0 mg of mixed anode powder was uniformly spread onto the surface of the bottom of the Swagelok cell; 2) 80 mg of solid electrolyte powder was spread onto the anode powder layer, followed by a light pressing at 70 MPa; 3) 3.4 mg of mixed cathode powder was spread uniformly onto the pressed solid electrolyte layer; 4) the three-layer pellet was finally fabricated under a pressure of 870 MPa. The whole process was conducted in an argon-filled glove box. The galvanostatic charge–discharge tests were conducted in a voltage rang of 2.5–4.2 V at 0.1 C to measure the electrochemical performances of ASSBs via a battery test system (Land, CT2001A) at 30 °C.

3. Results and discussion

3.1. Synthesis of Li_2S

As illustrated in Fig. 1(a), Li_2S was synthesized via liquid phase synthesis method, which is widely recognized as a cost-effective method for mass production with mild reaction conditions.[22] The Li metals can react with biphenyl in the DME solvent to form a dark green lithium solution at room temperature. This kind of solutions has been known as radical anions, acting as reducing agents in chemical synthesis since 1930s.[20,21] Because of its comparatively strong reducibility, it can react with sulfur at high reaction kinetics even at room temperature.

The XRD pattern of the as-synthesized Li_2S with a heat treatment at 250 °C is shown in Fig. 2(a), corresponding well with the indexed diffraction pattern of the Li_2S phase (PDF#00-023-0369) without impurity phase. The solvent used in the Li_2S synthesis was replaced by THF for comparison, with which the final product also exhibited the characteristic peaks of Li_2S. However, the peak intensity is lower compared with that of Li_2S mediated by DME solvent.

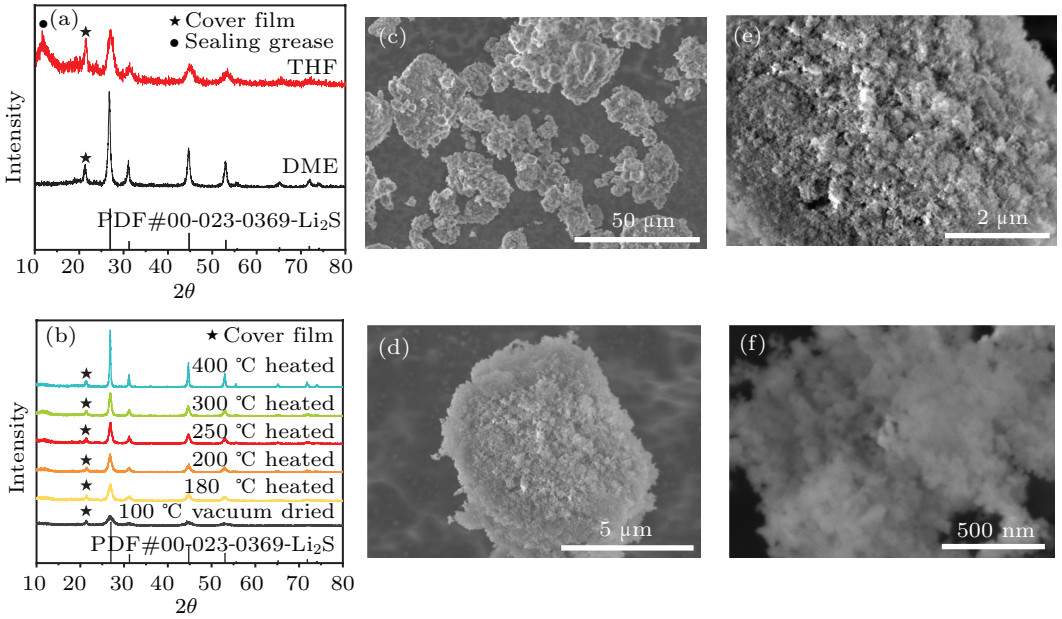


Fig. 2. (a) XRD patterns of the obtained Li_2S samples prepared by DME and THF, and the indexed diffraction pattern of the Li_2S phase (PDF#00-023-0369). (b) XRD patterns of the obtained Li_2S samples before and after heat treatment at different temperatures from 180 °C to 400 °C. (c)–(f) Morphology of the obtained Li_2S at 300 °C.

The Li_2S samples using DME solvent before and after heat treatment at different temperatures are shown in Fig. 2(b). The sample before heat treatment (after vacuum drying at 100 °C) shows characteristic peaks of Li_2S with low intensity, indicating the removal of DME at low temperature. For the samples after heat treatment at a series of temperatures from 180 °C to 400 °C, all diffraction peaks correspond well to the indexed diffraction pattern of the Li_2S phase, and become sharper with higher intensity, indicating that the cubic crystalline Li_2S phase has been formed. Interestingly, the particle size of the as-synthesized Li_2S is extremely small, as illustrated in the SEM images of Li_2S synthesized at 300 °C (Figs. 2(c)–2(f)). Figures 2(c) and 2(d) show the macroscopic morphology of Li_2S particles. Big agglomerates were observed (approximately 5–40 μm), which are composed of individual regular particles lower than 50 nm (Figs. 2(e) and 2(f)). The uniform and extremely small particle size should be attributable to the mediation of solvent during liquid-phase synthesis process.[15,23,24] The as-synthesized Li_2S with extremely small particle size can be a promising cathode material

for lithium-sulfur batteries, considering the critical role of particle size reduction in improving the reversibility and cycling stability of Li_2S cathode with insulating nature.[25–27]

The cost of Li_2S per kilogram (kg) synthesized via the liquid-phase synthesis route in this work and two conventional routes were roughly calculated and compared in Table 1, including materials cost and processing cost. It is noting that the cost of biphenyl and DME solvent in the liquid-phase synthesis route, and N-methyl-2-pyrrolidone (NMP) solvent in the synthesis route using LiOH and H_2S were neglected, considering their recyclability. The cost of Li_2S synthesized via the liquid-phase synthesis route in this work is calculated to be 947.885 RMB/kg, lower than that of the Li_2S synthesized via two conventional routes.

Table 1. Rough calculation of the cost of Li_2S per kilogram (kg) synthesized via the liquid-phase synthesis route in this work and two conventional routes.[a]

Cost of Li_2S synthesized via the liquid-phase method			
Raw materials	Quantity (kg/kg)	Price (RMB/kg)	Cost (RMB/kg)
Li	0.304	3000.000	912.000
S	0.695	43.000	29.885
Materials cost			941.885
Processing procedures	Energy consumption (kWh/kg)	Price (RMB/kWh)	Cost (RMB/kg)
Solvent recovery	10	0.6	6
Processing cost			6
Total cost			947.885
Cost of Li_2S synthesized via the carbothermic reduction of Li_2SO_4			
Raw materials	Quantity (kg/kg)	Price (RMB/kg)	Cost (RMB/kg)
Li_2SO_4	2.391	400.000	956.522
C	0.522	4.300	2.244
Materials cost			958.765
Processing procedures	Energy consumption (kWh/kg)	Price (RMB/kWh)	Cost (RMB/kg)
Ball milling	10	0.6	6
Sintering (at 900 °C for 5 h)	250	0.6	150
Processing cost			210
Total cost			1168.765
Cost of Li_2S synthesized via the reaction between LiOH and H_2S			
Raw materials	Quantity (kg/kg)	Price (RMB/kg)	Cost (RMB/kg)
LiOH	1.043	884.452	922.484
H_2S	0.739	37.800	27.934
Materials cost			950.418
Processing procedures	Energy consumption (kWh/kg)	Price (RMB/kWh)	Cost (RMB/kg)
Heating (at 200 °C for 5 h)	40	0.6	24
Solvent recovery	100	0.6	60
Processing cost			84
Total cost			1034.418

[a]Prices of raw materials and electricity were taken from the current market prices in China on May 25th, 2022.

To further investigate the feasibility of the as-synthesized Li_2S in synthesizing sulfide electrolyte, Li_6PS_5Cl solid electrolytes were synthesized and compared via conventional solid-state synthesis method using Li_2S synthesized at 300 °C and commercial Li_2S, respectively. As illustrated in Fig. 3(a), the XRD patterns of Li_6PS_5Cl solid electrolytes using synthesized Li_2S and purchased Li_2S are virtually the same, corresponding well with characteristic peaks of Li_6PS_5Cl and without any obvious impurity.

The electrochemical properties of the synthesized Li_6PS_5Cl solid electrolytes were also compared, using SS/cold-pressing Li_6PS_5Cl pellet/SS cells with SS rods as the ion-blocking electrodes (Figs. 3(a) and 3(b), Table 2). The Nyquist plots at 30 °C for two kinds of Li_6PS_5Cl are shown in Fig. 3(b), exhibiting only one line in low frequency region for both plots, representing the Warburg diffusion impedance (W). The absence of semicircles in the high frequency region representing the bulk resistance ($R_{SE,bulk}$) of solid electrolyte and in the intermediate frequency region representing the grain boundary resistance ($R_{SE,gb}$) of solid electrolyte indicates the relatively small resistance of the solid electrolyte. The inset in Fig. 3(b) shows the corresponding equivalent circuit of Nyquist plot. The ionic conductivity is calculated from the total resistance ($R_{SE,total} = R_{SE,bulk} + R_{SE,gb}$) after cold-pressing at 870 MPa, which is obtained from the intercept of line in the low frequency region of x-axis. The as-calculated

total ionic conductivity for Li_6PS_5Cl solid electrolytes synthesized using synthesized Li_2S is 4.57×10^{-3} S·cm^{-1} at 30 °C, slightly lower than that of Li_6PS_5Cl obtained using commercial Li_2S (6.03×10^{-3} S·cm^{-1}). This might because of the XRD-undetectable amounts of impurity phases.

The DC polarization technique was employed to the SS/cold-pressing Li_6PS_5Cl pellet/SS cells to measure the electronic conductivity of Li_6PS_5Cl solid electrolyte. Figure 3(c) shows the time dependence of the current under a polarization voltage of 50 mV. The electronic resistances were obtained from the steady-state current value after the application of the voltage of 50 mV for 600 s. Based on the DC curves, the calculated electronic conductivities of synthesized Li_6PS_5Cl solid electrolytes using synthesized Li_2S and commercial Li_2S are 4.45×10^{-9} S·cm^{-1} and 6.67×10^{-9} S·cm^{-1}, respectively, consistent with the previously reported values of electronic conductivity for Li_6PS_5Cl solid electrolyte (10^{-9} S·cm^{-1}).[28–30]

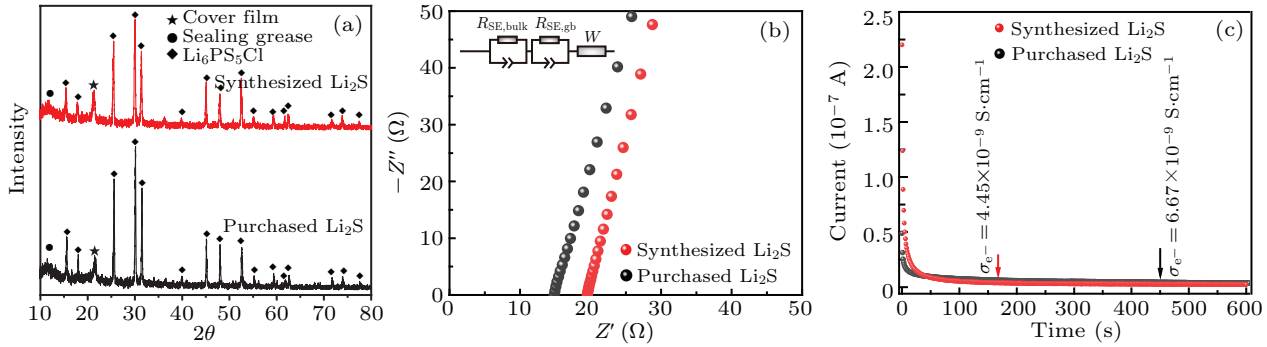


Fig. 3. (a) XRD patterns of the synthesized Li_6PS_5Cl solid electrolytes via conventional solid-state synthesis method using synthesized Li_2S at 300 °C and purchased Li_2S. (b) Nyquist plots and (c) chronoamperometry profiles under a polarization voltage of 50 mV of SS/Li_6PS_5Cl/SS cells using synthesized Li_6PS_5Cl solid electrolytes via conventional solid-state synthesis method employing synthesized Li_2S and purchased Li_2S. The equivalent circuit is inserted in the Nyquist plots, in which $R_{SE,bulk}$ is the volume resistance of the solid electrolyte, $R_{SE,gb}$ is the grain boundary resistance of the solid electrolyte, and W is the Warburg impedance.

Table 2. Summary of the ionic conductivity (σ_{Li^+}) and electronic conductivity (σ_{e^-}) at 30 °C of the synthesized Li_6PS_5Cl solid electrolytes via conventional solid-state synthesis method using Li_2S synthesized at 300 °C and commercial Li_2S.

Li_6PS_5Cl samples	σ_{Li^+} at 30 °C (S·cm^{-1})	σ_{e^-} at 30 °C (S·cm^{-1})
Synthesized Li_2S	4.57×10^{-3}	4.45×10^{-9}
Purchased Li_2S	6.03×10^{-3}	6.67×10^{-9}

NCM811/Li_6PS_5Cl/Si lab-scale ASSBs using the synthesized Li_6PS_5Cl via conventional solid-state synthesis method using liquid-phase-synthesized Li_2S and purchased Li_2S were assembled and compared to evaluate the feasibility of the as-synthesized Li_2S in synthesizing Li_6PS_5Cl sulfide solid electrolytes. As illustrated in Fig. 4(a), the two batteries exhibit comparable charge and discharge profiles. The ASSBs using the Li_6PS_5Cl synthesized via liquid-phase-synthesized Li_2S delivers a reversible discharge capacity of 174.2 mAh·g^{-1} and a Coulombic efficiency of 66.33% at the 1st cycle, while the ASSBs using the Li_6PS_5Cl synthesized via purchased Li_2S delivers a reversible discharge capacity of 170.0 mAh·g^{-1} and a Coulombic efficiency of 65.50% under the same test conditions. Furthermore, the battery with the Li_6PS_5Cl synthesized via liquid-phase-synthesized Li_2S delivers good cycling performance, as shown in Figs. 4(b) and 4(c). The overpotentials of profiles increase gradually during cycling, corresponding to discharge capacities of 167.7, 161.6, 154.3, 134.7, 113.9 and 104.6 mAh·g^{-1} at the 5th, 10th, 20th, 50th, 80th and 100th cycle, respectively. To conclude, the as-synthesized Li_6PS_5Cl exhibits satisfactory compatibility with NCM811/Si system. Therefore, the as-synthesized Li_2S can be successfully employed in synthesizing sulfide solid electrolytes.

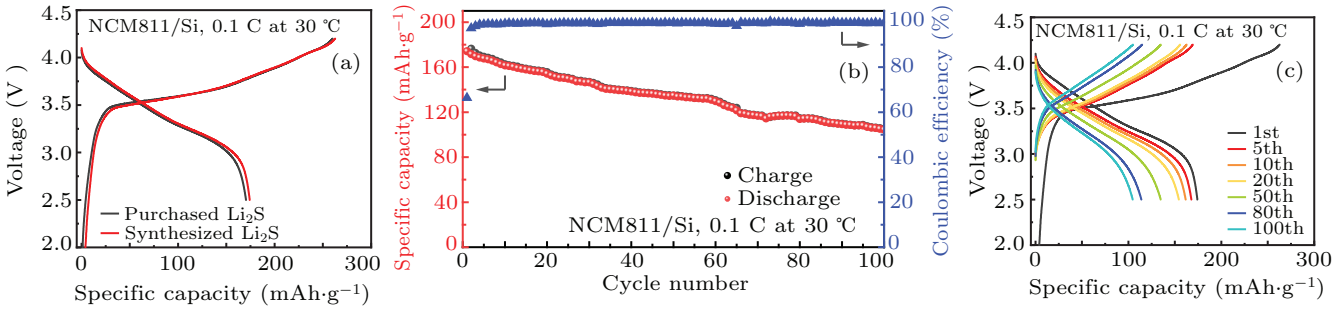


Fig. 4. (a) Charge and discharge profiles at the 1st cycle of NCM811/Li_6PS_5Cl/Si lab-scale ASSBs using the synthesized Li_6PS_5Cl via conventional solid-state synthesis method using liquid-phase-synthesized Li_2S and purchased Li_2S, respectively. (b), (c) Cycling performances of NCM811/Li_6PS_5Cl/Si lab-scale ASSBs using the synthesized Li_6PS_5Cl via conventional solid-state synthesis method using liquid-phase-synthesized Li_2S. (b) Cycling performances (0.1 C, 1 C=200 mA·g^{-1}, in the voltage range of 2.5–4.2 V). (c) Charge and discharge profiles of ASSBs at the typical cycles.

3.2. Synthesis of Li_3PS_4

The application of $Li_{1.0}Bp_{1.0}(DME)_{1.0}$ lithium solution in Li_2S synthesis has been proved to be feasible in synthesizing sulfide solid electrolytes (such as the solid-state synthesis of Li_6PS_5Cl) in the front part. The direct employment of lithium solution in Li_3PS_4 solid electrolytes via liquid-phase synthesis was also investigated in this work, in which the centrifugation and heat treatment processes of Li_2S are not necessary, providing simplified production process.

For this purpose, two synthesis routes can be possible, as illustrated in Fig. 1(b). For the two-step route, sulfur first reacted with lithium solution to form the suspension of Li_2S in Bp-DME solution, followed by the reaction between P_2S_5 and Li_2S with the addition of P_2S_5. For the one-step route, the synthesis process is further simplified, in which sulfur and P_2S_5 reacted with lithium solution at the same time.

Following the two-step route, Li_3PS_4 solid electrolytes were synthesized employing different solvents (DME and THF) and different heat treatment temperatures (160–250 °C) to optimize the synthesis parameters. First, different solvents were respectively employed in the synthesis of Li_3PS_4 at heat treatment of 250 °C to determine the suitable solvent. Figure 5(a) displays the XRD patterns of resulting products using DME and THF. The XRD pattern of the resulting product using DME solvent corresponds well with the indexed diffraction pattern of the Li_3PS_4 phase (PDF#01-076-0973) without any impurity phase, indicating the successful synthesis of Li_3PS_4. For the THF solvent, which is widely employed in the synthesis of Li_3PS_4 via liquid-phase synthesis method,[12,14,31] except for the Li_3PS_4 phase, the S_8 phase was also detected. This might be due to the insufficient dissolution or reactivity of lithium in Bp-THF solution. Therefore, DME solvent is suitable for the synthesis of Li_3PS_4. Figure 5(b) shows the XRD patterns of Li_3PS_4 samples using DME solvent before and after heat treatment at a series of temperatures from 160 °C to 250 °C. The sample before heat treatment (after vacuum drying at 100 °C for 12 h) is well-crystallized because of the complex formation with DME,[32] and the DME solvent can not be removed after heat treatment at 160 °C. For the samples after heat treatment at a series of temperatures from 170 °C to 250 °C, all diffraction peaks correspond well to the indexed diffraction pattern of the Li_3PS_4 phase without any impurity or formation of new phase. Considering the almost unchanged peak sharpness and intensity from 180 °C, 180 °C was fixed as the optimal heat treatment temperature for further study.

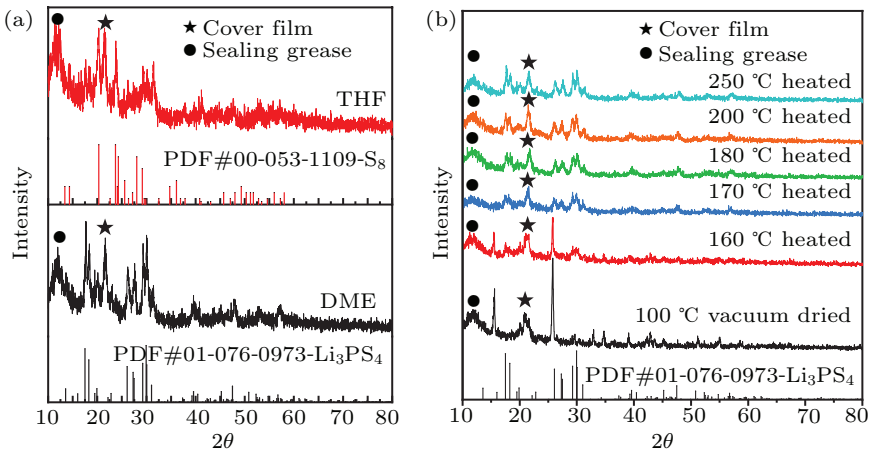


Fig. 5. (a) XRD patterns of the obtained Li_3PS_4 samples prepared by DME and THF, and the indexed diffraction pattern of the Li_3PS_4 phase (PDF#01-076-0973) and the S_8 phase (PDF#00-053-1109). (b) XRD patterns of the obtained Li_3PS_4 samples before and after heat treatment at different temperatures from 160 °C to 250 °C.

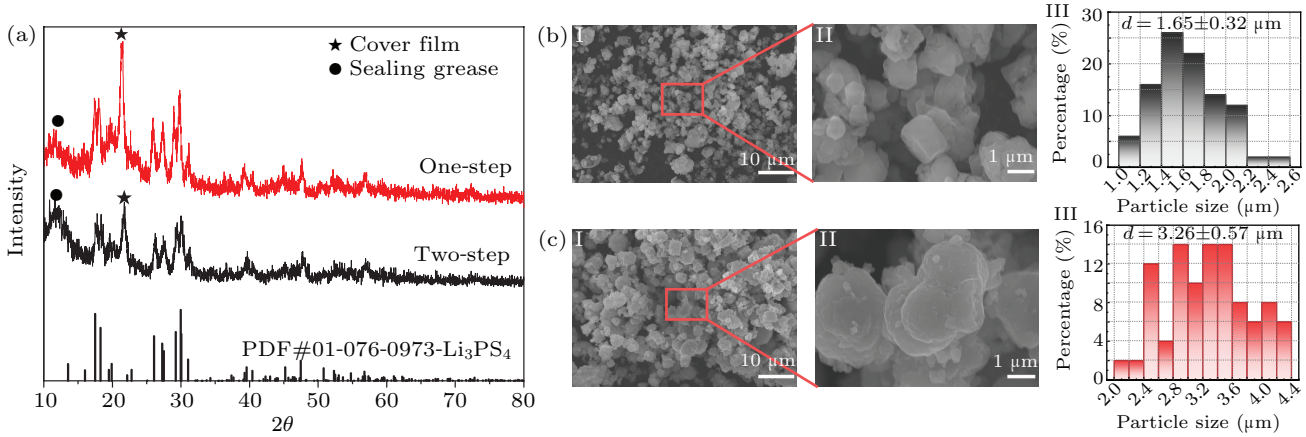


Fig. 6. (a) XRD patterns of the obtained Li_3PS_4 samples prepared by two-step and one-step routes, and the indexed diffraction pattern of the Li_3PS_4 phase (PDF#01-076-0973). (b), (c) Morphology and corresponding particle size distribution of the obtained Li_3PS_4 samples prepared by (b) two-step and (c) one-step routes.

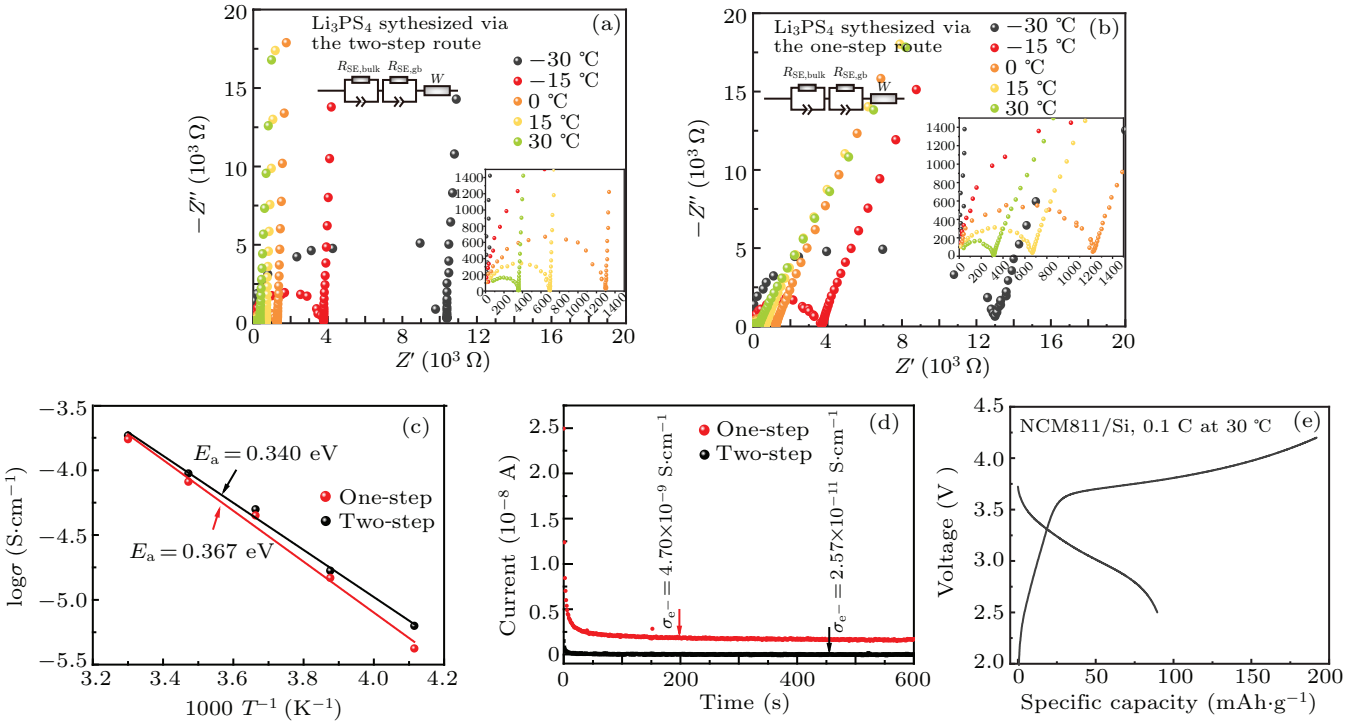


Fig. 7. (a) Nyquist plots of SS/Li_3PS_4/SS cells at temperatures from −30 °C to 30 °C using synthesized Li_3PS_4 solid electrolytes via (a) two-step route and (b) one-step route. Insert: the magnified region and the corresponding equivalent circuit of the Nyquist plots. (c) Arrhenius plots of synthesized Li_3PS_4 solid electrolytes via two-step and one-step routes. (d) Chronoamperometry profiles under a polarization voltage of 50 mV of the SS/Li_3PS_4/SS cells using synthesized Li_3PS_4 solid electrolytes via two-step and one-step routes. (e) Charge and discharge profiles at the 1st cycle of the NCM811/Li_3PS_4/Si lab-scale ASSB using the synthesized Li_3PS_4 via the two-step route.

The two synthesis routes including two-step and one-step routs were compared, using DME as the solvent and heat treatment at 180 °C. In both cases, pure-phase Li_3PS_4 was obtained via the detection of XRD (Fig. 6(a)). The difference in particle size was observed, as illustrated in Figs. 6(b) and 6(c). The two-step synthesized Li_3PS_4 exhibits uniform particle size of 1.65±0.32 μm, smaller that of one-step-synthesized Li_3PS_4 (3.26±0.75 μm). This might be attributable to the relatively adequate and uniform chemical reaction during solvent-solid interactions in the two-step synthesis process.

The electrochemical performances of the synthesized Li_3PS_4 via two routes were also compared (Fig. 7 and Table 3). Figures 7(a) and 7(b) show the Nyquist plots of SS/Li_3PS_4/SS cells at temperatures from −30 °C to 30 °C using synthesized Li_3PS_4 solid electrolytes via two routes. The plots bothe consist of a semicircle and a spike. The line in the low frequency region represents the diffusion impedance (W), and the incomplete semicircle contains the the grain boundary resistance ($R_{SE,gb}$) of the solid electrolyte in the intermediate frequency region and the bulk resistance ($R_{SE,bulk}$) of the solid electrolyte in the high frequency region. The corresponding equivalent circuit is illustrated as the insert in Nyquist plots. The intercept of the semicircle in the intermediate frequency region of x-axis, recognized as the total resistance ($R_{SE,total} = R_{SE,bulk} + R_{SE,gb}$) after cold-pressing at 870 MPa, gradually decreases with the increase of temperature, indicating the increase of Li^+ conductivity. As illustrated in Fig. 7(c), the as-calculated Li^+ conductivities of the synthesized Li_3PS_4 via two routes all conform to the Arrhenius equation

$$\sigma = A\exp\left(\frac{-E_a}{kT}\right),$$

where E_a is the activation energy for Li^+ conduction, A is the pre-exponential factor, and k is the Boltzmann constant. The two-step synthesized Li_3PS_4 exhibited a Li^+ conductivity of 1.85×10^{-4} S·cm^{-1} at 30 °C and an Arrhenius activation energy of 0.340 eV, while the one-step synthesized Li_3PS_4 exhibited a Li^+ conductivity of 1.74×10^{-4} S·cm^{-1} at 30 °C and an Arrhenius activation energy of 0.367 eV, consistent with the previously reported values of liquid-phase synthesized Li_3PS_4.[31,33] Figure 7(d) shows the time dependence of the current under a polarization voltage of 50 mV, and the calculated electronic conductivities of the synthesized Li_3PS_4 solid electrolytes via two-step and one-step routes are 2.57×10^{-11} S·cm^{-1} and 4.70×10^{-9} S·cm^{-1}, respectively. To conclude, although the two-step synthesis route requires longer synthesis time compared with the one-step route, the as-synthesized Li_3PS_4 exhibited better electrochemical performances and small particle size, which is supposed to provide ASSBs with preferable electrochemical performances. NCM811/Li_3PS_4/Si lab-scale ASSBs using the synthesized Li_3PS_4 via the two-step route were assembled and tested to evaluate the compatibility of the as-synthesized Li_3PS_4 with NCM811/Si system (Fig. 7(e)). The battery exhibits a reversible capacity of 89.5 mAh·g^{-1} with large polarization for

the 1st cycle, which should be attributable to the relatively lower ionic conductivity of Li_3PS_4 compared with Li_6PS_5Cl.

Table 3. Summary of the ionic conductivity (σ_{Li^+}) and electronic conductivity (σ_{e^-}) of the synthesized Li_3PS_4 via two-step and one-step routes at 30 °C.

Li_3PS_4 samples	σ_{Li^+} at 30 °C (S·cm^{-1})	σ_{e^-} at 30 °C (S·cm^{-1})
Two-step	1.85×10^{-4}	2.57×10^{-11}
One-step	1.74×10^{-4}	4.70×10^{-9}

4. Conclusion and perspectives

In conclusion, a new synthesis route of Li_2S via liquid-phase synthesis method was developed in this work, using lithium solution with strong reducibility as lithium precursor. This new synthesis route of Li_2S starts with cheap precursors of lithium, sulfur, biphenyl and DME solvent, and the only remaining byproduct (DME solution of biphenyl) after the collection of Li_2S product can be recycled and reused. Besides, the reaction can proceed effectively at room temperature with mild condition, reducing energy cost to a great extent. The as-synthesized Li_2S owns uniform and extremely small particle size, proved to be feasible in synthesizing sulfide solid electrolytes (such as the solid-state synthesis of Li_6PS_5Cl). Spontaneously, this lithium solution can be directly employed in the synthesis of Li_3PS_4 solid electrolytes via liquid-phase synthesis method, in which the centrifugation and heat treatment processes of Li_2S are not necessary, providing simplified production process. The synthesis parameters of Li_3PS_4, including the solvent type, heat treatment temperature and route were systematically investigated. The as-synthesized Li_3PS_4 with the optimal parameters (using DME solvent, with heat treatment at 180 °C via two-step route) exhibits typical Li^+ conductivity of 1.85×10^{-4} S·cm^{-1} at 30 °C.

Acknowledgements

This work is supported by Key R&D Project funded by Department of Science and Technology of Jiangsu Province (Grant No. BE2020003), Key Program-Automobile Joint Fund of National Natural Science Foundation of China (Grant No. U1964205), General Program of National Natural Science Foundation of China (Grant No. 51972334), General Program of National Natural Science Foundation of Beijing (Grant No. 2202058), Cultivation Project of Leading Innovative Experts in Changzhou City (Grant No. CQ20210003), National Overseas High-level Expert Recruitment Program (Grant No. E1JF021E11), Talent Program of Chinese Academy of Sciences, "Scientist Studio Program Funding" from Yangtze River Delta Physics Research Center and Tianmu Lake Institute of Advanced Energy Storage Technologies (Grant No. TIES-SS0001), and Science and Technology Research Institute of China Three Gorges Corporation (Grant No. 202103402).

References

[1] Liu L, Xu J, Wang S, Wu F, Li H and Chen L 2019 *eTransportation* **1** 100010
[2] Kanno R and Murayama M 2001 *J. Electrochem. Soc.* **148** A742
[3] Kamaya N, Homma K, Yamakawa Y, Hirayama M, Kanno R, Yonemura M, Kamiyama T, Kato Y, Hama S, Kawamoto K and Mitsui A 2011 *Nat. Mater.* **10** 682
[4] Kato Y, Hori S, Saito T, Suzuki K, Hirayama M, Mitsui A, Yonemura M, Iba H and Kanno R 2016 *Nat. Energy* **1** 16030
[5] Sakuda A 2018 *J. Ceram. Soc. Jpn.* **126** 675
[6] Hayashi A, Hama S, Minami T and Tatsumisago M 2003 *Electrochem. Commun.* **5** 111
[7] Seino Y, Nakagawa M, Senga M, Higuchi H, Takada K and Sasaki T 2015 *J. Mater. Chem. A* **3** 2756
[8] Ohara K, Mitsui A, Mori M, Onodera Y, Shiotani S, Koyama Y, Orikasa Y, Murakami M, Shimoda K, Mori K, Fukunaga T, Arai H, Uchimoto Y and Ogumi Z 2016 *Sci Rep* **6** 21302
[9] Minami K, Mizuno F, Hayashi A and Tatsumisago M 2007 *Solid State Ionics* **178** 837
[10] Hayashi A, Yamashita H, Tatsumisago M and Minami T 2002 *Solid State Ionics* **148** 381
[11] Kim Y and Martin S 2006 *Solid State Ionics* **177** 2881
[12] Liu Z, Fu W, Payzant E A, Yu X, Wu Z, Dudney N J, Kiggans J, Hong K, Rondinone A J and Liang C 2013 *J. Am. Chem. Soc.* **135** 975
[13] Wang H, Hood Z D, Xia Y N and Liang C D 2016 *J. Mater. Chem. A* **4** 8091
[14] Hood Z D, Wang H, Pandian A S, Peng R, Gilroy K D, Chi M F, Liang C D and Xia Y N 2018 *Adv. Energy Mater.* **8** 1800014
[15] Choi S, Lee S, Park J, Nichols W T and Shin D 2018 *Appl. Surf. Sci.* **444** 10
[16] Bertau M, Müller A, Fröhlich P, Katzberg M, Büchel K H, Moretto H-H and Werner 2013 *Industrielle Anorganische Chemie*, 4th edn. (Weinheim: Wiley-VCH)
[17] Kazutomi Y and Nobuhiko I (E.P.) 0802159B1 [1997-04-14]
[18] Yoshikatsu S and Minoru S (E.P.) 1681263B1 [2004-10-15]
[19] Schlenk W and Bergmann E 1928 *Justus Liebigs Ann. Chem.* **463** 1
[20] Scott N D, Walker J F and Hansley V L 1936 *J. Am. Chem. Soc.* **58** 2442
[21] Connelly N G and Geiger W E 1996 *Chem. Rev.* **96** 877
[22] Xu R, Yue J, Liu S, Tu J, Han F, Liu P and Wang C 2019 *ACS Energy Lett.* **4** 1073
[23] Phuc N H H, Morikawa K, Totani M, Muto H and Matsuda A 2016 *Solid State Ionics* **285** 2
[24] Phuc N H H, Morikawa K, Mitsuhiro T, Muto H and Matsuda A 2017 *Ionics* **23** 2061
[25] Cai K, Song M K, Cairns E J and Zhang Y 2012 *Nano Lett.* **12** 6474
[26] Nan C, Lin Z, Liao H, Song M K, Li Y and Cairns E J 2014 *J. Am. Chem. Soc.* **136** 4659
[27] Suo L, Zhu Y, Han F, Gao T, Luo C, Fan X, Hu Y S and Wang C 2015 *Nano Energy* **13** 467
[28] Wang S, Zhang Y, Zhang X, Liu T, Lin Y H, Shen Y, Li L and Nan C W 2018 *ACS Appl. Mater. Interfaces* **10** 42279
[29] Zhao F, Sun Q, Yu C, Zhang S, Adair K, Wang S, Liu Y, Zhao Y, Liang J, Wang C, Li X, Li X, Xia W, Li R, Huang H, Zhang L, Zhao S, Lu S and Sun X 2020 *ACS Energy Lett.* **5** 1035
[30] Koç T, Marchini F, Rousse G, Dugas R and Tarascon J M 2021 *ACS Appl. Energy Mater.* **4** 13575
[31] Lim H D, Yue X J, Xing X, Petrova V, Gonzalez M, Liu H D and Liu P 2018 *J. Mater. Chem. A* **6** 7370
[32] Ito S, Nakakita M, Aihara Y, Uehara T and Machida N 2014 *J. Power Sources* **271** 342
[33] Phuc N H H, Totani M, Morikawa K, Muto H and Matsuda A 2016 *Solid State Ionics* **288** 240